Comparison of Direct Voltage Control Methods of Multi-Terminal DC (MTDC) Networks through Modular Dynamic Models

R. Teixeira Pinto	S. F. Rodrigues	P.Bauer	J. Pierik
TU Delft	IST Lisboa	TU Delft	ECN
Mekelweg, 4	Av. Rovisco Pais, 1	Mekelweg, 4	Westerduinweg, 34
Delft, Netherlands	Lisbon, Portugal	Delft, Netherlands	Petten, Netherlands
r.teixeirapinto@tudelft.nl	silviorodrigues@ist.utl.pt	p.bauer@tudelft.nl	pierik@ecn.nl

Acknowledgements

This paper is part of the North Sea Transnational Grid project, which is financially supported by the EOS research program of the Netherlands, executed by the Agentschap NL of the Ministry of Economic Affairs, Agriculture and Innovation.

Keywords

Multi-terminal HVDC, Voltage Source Converter (VSC), Wind energy, Control methods for electrical systems, power transmission.

Abstract

Estimates are that circa 40GW of offshore wind power capacity is going to be installed throughout Europe by the end of this decade. In this scenario, a pan-European offshore grid network is needed in order to efficiently integrate large amounts of offshore wind into the different European countries' transmission networks. In this paper, the dynamic model of multi-terminal HVDC (MTDC) transmission system composed of voltage-source converters is presented. Afterwards, the dynamic models are used to compare four different methods for controlling the DC voltage inside MTDC networks, viz.: droop control, ratio control, priority control and voltage margin control. Lastly, a case study is performed in a four-node MTDC network and the different control strategies are compared.

Introduction

Dynamic models of future large offshore multi-terminal DC networks are needed for assessment of the overall system behaviour during steady-state, transients and fault conditions; but also for control designing purposes. If the dynamic model is modular, the highly complex systems can be divided into smaller sub-modules. In that way, the complete system model can easier evolve with time. In addition, using modular dynamic models makes it easier to perform comparative tests of individual modules performance, such as different wind turbines or HVDC technologies.

To model large offshore transnational grids, the approach is to derive the differential equations for the dynamic models of the most important modules inside the system, viz.: wind farms, HVDC stations, the multi-terminal DC grid and the onshore AC systems. With this modular approach, it will be possible to study the dynamic behaviour of MTDC networks irrespective of their topology.

MTDC Network Dynamic Model

Multi-terminal HVDC (MTDC) transmission systems are characterized by more than two HVDC converter stations somehow interconnected on the DC side of the transmission system [1]. The MTDC configurations can be classified according to the type of HVDC technology implemented at the converter stations, i.e.: line-commutated current-source converters (CSC) or forced-commutated voltage-source converters (VSC) or eventually a combination of both technologies.

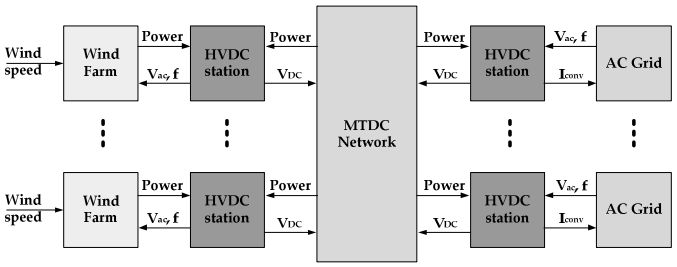

Fig. 1: Modular representation of an offshore MTDC network.

Even though there are over one hundred HVDC transmission systems installed all over the world, only three schemes have more than two terminals [2][3]. Fig.1 shows the layout of a MTDC network with more than two terminals. In order to solve the electrical equations of the MTDC network, it is necessary to know the DC voltage of all the nodes inside the system. Then, with knowledge of the DC voltages of all the HVDC stations it is possible to evaluate the DC current flowing in each of the transmission system's lines since:

$$\mathbf{I}_L = \mathbf{Y}(s) \cdot \mathbf{V}_{DC} \tag{1}$$

where **Y**(s) is the MTDC network admittance matrix, which is dependent on the topology of the MTDC grid.

After calculating the DC current in all lines of the MTDC system, the power flowing in the lines can be computed as:

$$P_L^n = I_L^n \cdot V_{DC}^n \tag{2}$$

where *n* is the station index number.

VSC-HVDC Dynamic Model

Given the characteristics of VSC-HVDC transmission systems it is most probable that this technology will be the one initially chosen for the connection of large offshore wind farms since in offshore projects the converter station footprint is a critical variable. Modern state-of-the-art voltage-source converters for transmission purposes make use of modulation schemes or multilevel topologies, which allow them to have smaller space requirements than current-source converters.

The VSC-HVDC model here presented is modular and composed of several modules, viz.: a phase reactor, an inner current controller, the converter model, the outer controllers and the station capacitor. The signal flow inside the model is shown in Fig. 2.

Phase Reactor

A phase reactor is generally installed on the AC side of the VSC station. The reactor helps to further reduce AC high-frequency harmonic content, caused by the switching of the converter valves. In addition, independent control of active and reactive power is accomplished by regulating the voltage drop and current flow through the phase reactor on each converter station. On the AC network side, the dynamics of the VSC-HVDC are modelled, in the rotating coordinate *(dq)* frame, by the following state-space equation:

$$L_T \frac{d}{dt}\left(\bar{i}_{dq}\right) = \bar{e}_{dq} - \bar{v}_{dq} - R_T \bar{i}_{dq} - \mathbf{j}\omega L_T \bar{i}_{dq} \tag{3}$$

The system resulting from (3) is linear and autonomous, i.e. does not depend on time as an independent variable, if ω is constant. The poles of the system represented in (3) will be given by the roots of $\left(s + R_T / L_T\right)^2 + \omega^2 = 0$ .For $\omega = 2\pi f$, where *f* is the AC network frequency (50 or 60 Hz), the poles of the non-feed-backed VSC system will be oscillatory. Moreover, without feedback of the converter currents the system would be poorly damped and have a very bad dynamic performance (under-damped response).

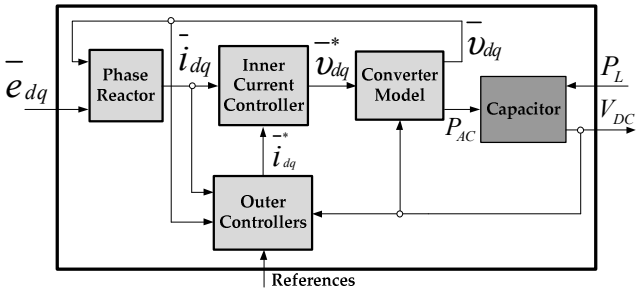

Fig. 2: Modular representation of the VSC-HVDC transmission station.

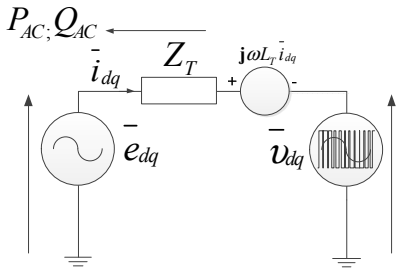

Fig. 3 VSC-HVDC station single-phase equivalent circuit.

Inner Current Controller

The solution to improve the VSC system performance is to feedback the converter current through a controller closing the current loop. The block diagram representation of the VSC-HVDC with feedback control is displayed below in Fig. 4. Initially considering the controller to be a simple proportional gain, i.e. $C(s) = K_p$, the block diagram presented can be simplified by solving the outer feedback loops. With the assumption that $K_p >> R_T$, the equivalent block diagram representation of the system with the proportional controller becomes the one shown in Fig. 5.

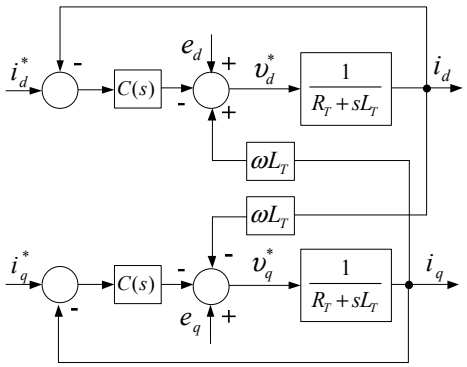

Fig. 4: Block diagram representation of the VSC state-space equations with feedback control.

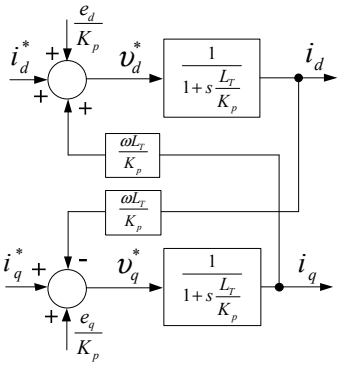

Fig. 5: Equivalent block diagram representation of the VSC.

With reference to the equivalent diagram (Fig. 5) it is possible to derive the following transfer function for the converter current in the q-axis (the same apply for the d-axis):

$$\frac{i_q}{i_q^*} = \frac{1 + sL_T / K_p}{\left(\omega L_T / K_p\right)^2 + \left(1 + sL_T / K_p\right)^2} \approx \frac{1}{1 + sL_T / K_p} \tag{4}$$

Therefore, having a sufficiently high proportional gain in the closed-loop controller not only improves the system response but also helps, in steady state, to eliminate the cross-coupled interaction between the d-axis and q-axis. Since during steady state s=0, it follows:

$$\frac{i_q}{i_q^*} = \frac{1}{\left(\omega L_T / K_p\right)^2 + 1} \approx 1 \;\; and \;\; \frac{i_q}{i_d^*} = \frac{\omega L_T / K_p}{\left(\omega L_T / K_p\right)^2 + 1} \approx \omega L_T / K_p \tag{5}$$

In fact, if $\omega L_T / K_p << 1$, the cross-coupling influence among the axes are cancelled out. Thus, starting from the oscillatory system of (3), by adding a proportional controller and closing the current-loop, the VSC-HVDC system now resembles two first-order systems (one for each axis) with poles in K_p / L_T, which is the closed-loop bandwidth, α_c, of the system.

For a satisfactory dynamic performance, the closed-loop bandwidth of the system should not be higher than 5 times the angular switching frequency [4]. In this way, the value of the maximum proportional gain, K_p, is fixed by the maximum obtainable inner current control bandwidth. It follows that, in the VSC model, in order to obtain the desired closed-loop bandwidth it is sufficient to make $K_p = \alpha_c L_T$.

Nevertheless, the proportional gain is limited due to the switching frequency limitation. Hence, there will be a small error in the inner current controller, determined by $(\omega L_T/K_p)^2$ in the denominator of (5), in steady state. To cancel the steady-state error the solution is to use a PI regulator:

$$\overline{v}_{dq}^{*} = \overline{e}_{dq} - \left(K_p + \frac{K_i}{s} \right) \left(\overline{i}_{dq}^{*} - \overline{i}_{dq} \right) - \mathbf{j}\omega L_T \overline{i}_{dq} \tag{6}$$

As the steady-state error is only a few percentage, the integrator gain, K_i, can be low.

Converter Model

The next block inside the dynamic model of the VSC-HVDC is the model of the converter itself. Since the closed-loop bandwidth of the current controller is usually circa 5 times the converter switching frequency, its dynamic behaviour can be neglected when evaluating the dynamic response of MTDC systems as a whole. For this reason usually the average model of the converter is used, i.e.:

$$\overline{v}_{dq}(k+1) = \overline{v}_{dq}^{*}(k) \tag{7}$$

where one time-step delay is introduced due to the controller computational time and also due to the converter blanking time [5].

VSC-HVDC Station Capacitor

On the DC side, the VSC-HVDC station is usually represented by a controllable current source, acting on the station capacitor, as represented in Fig. 6. The DC voltage of the VSC station and the power flowing into the DC network are then given by:

$$W_{DC}^{n} = \int \left(P_{DC}^{n} - P_{L}^{n} \right) dt = \frac{1}{2} C_n \left(V_{DC}^{n} \right)^2 \tag{8}$$

Outer Controllers

The outer controllers are the ones responsible for providing the current references signals for the inner current controller. If, under steady state, the q-axis of the *(dq)* frame is assumed to be aligned with the AC network voltage phasor through a PLL, i.e. $e_d = 0$, the active-power related controllers will provide i_q^* whilst the reactive-power ones will provide i_d^*. The following equations give the references values for the outer controllers:

$$\begin{cases} i_d^{*} = \left(q_{AC}^{*} - q_{AC} \right) \cdot \left(K_{pq} + K_{iq}/s \right) \ or \ i_d^{*} = \left(\left| e_{dq}^{*} \right| - \left| e_{dq} \right| \right) \cdot \left(K_{pv} + K_{iv}/s \right) \\ i_q^{*} = \left(p_{AC}^{*} - p_{AC} \right) \cdot \left(K_{pp} + K_{ip}/s \right) \ or \ i_q^{*} = \left(W_c^{*} - W_c \right) \cdot \left(K_{pw} + K_{iw}/s \right) \end{cases} \tag{9}$$

In all the outer controllers PI regulators are employed to annul steady-state errors. The DC-voltage outer controller is made to operate on the error proportional to the square of the DC voltage, ΔW_c, instead of directly on the direct voltage. This is done to avoid nonlinearities in the DC voltage controller. For stability reasons, the outer controllers must have slower dynamics than the current controller. A rule of thumb is that the outer controllers bandwidth should be kept at least 10% smaller than the current controller bandwidth [6].

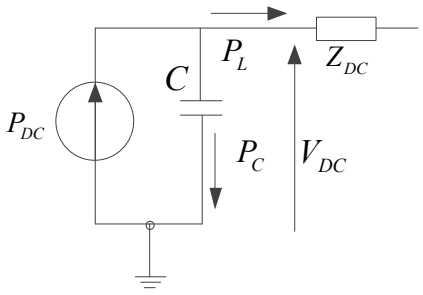

Fig. 6: Equivalent circuit of the VSC-HVDC station DC side.

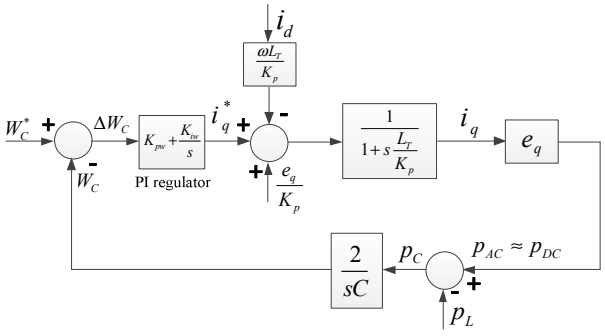

Fig. 7: Equivalent block diagram representation of the VSC with DC voltage and inner current controllers.

Direct Voltage Control Methods

Inside a multi-terminal DC network the direct voltage control is certainly one of the most important tasks given to the VSC-HVDC stations. A well-controlled DC voltage on a HVDC link is a guarantee of the power balance between all the interconnected nodes. If the DC voltage increases excessively, it may trigger protective equipment. On the other hand, a large DC voltage drop might generate non-linear phenomena, creating difficulties for the control systems, and can also temporarily limit the capability of the AC voltage controller [7].

Conventionally, in point-to-point HVDC transmission systems, one terminal controls the link's voltage while the other operates in current – or power – regulation mode. Inside a MTDC network, if the net sum of the active power of all the converters operating in current regulation mode is assured to be lower than the maximum ratings of the DC voltage controlling station, this traditional control scheme could be expanded for multi-terminal purposes.

However, controlling the MTDC network voltage at a single terminal is not desirable. In addition, if an outage would affect the only DC voltage controlling station, the fast nature of the phenomena in MTDC systems could trigger protection equipment, such as dump resistors, within only a few cycles of the AC network. Thus, sharing the task of controlling the DC voltage in the MTDC network among more than one converter station, in a distributed voltage regulation scheme, seems to be a much more effective way of operating the system.

Voltage Droop

The droop control strategy was firstly proposed for controlling CSC-MTDC networks [8]. However, this method can also be applied for VSC-MTDC networks [9]. The droop control scheme for MTDC networks works similar to the one implemented in traditional AC systems, where the load dependent frequency variation is used as an input signal for the control system to adjust the generated power to meet demand at all times. In MTDC networks the control employs the droop mechanism to regulate the DC voltage within the system by adjusting the converter current, as shown in Fig. 8[1], so that power balance is guaranteed.

The synchronization of the several VSC terminals happens without the need for fast communication between the terminals. If the network DC voltage starts increasing, there is power surplus in the system and the regulating stations should increase inversion. In the other hand, as the voltage starts to decrease, power is lacking in the system and the regulating stations should increase rectification.

In a similar way in which AC grids operate with regard to the transmission system operator grid code, offshore DC networks will also require rules. For instance, the droop control parameters – $V_{dc}(\min)$ and $V_{dc}(\max)$ – could also be established by such a standard. Examples of design rules for MTDC networks could include, but are not limited to, the DC voltage level (nominal, steady-state and transient range), the size and topology of each HVDC station, protection philosophy, control strategy and the power transfer capability of the DC cables.

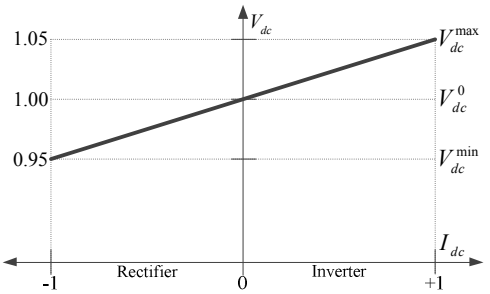

Fig. 8: MTDC droop controller.

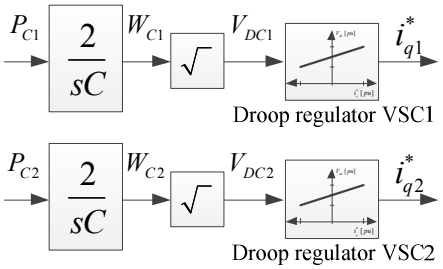

Fig. 9: Block representation of the droop control strategy.

[1] In practice, the droop regulator is implemented so that the maximum V_{dc} occurs at the maximum converter current. $p_{ac} = e_d i_d + e_q i_q \approx p_{dc} = v_{dc} i_{dc}$ since $e_d \approx 0; e_q \approx 1$ *and* $v_{dc} \approx 1 \Rightarrow i_q^* \approx i_{dc}^*$

Ratio Control

On this control strategy a power ratio between the two DC voltage controlling stations is established and the converters will then share the power generated by the wind parks according to this ratio [10]. The difference between the ratio controller and the droop controller is that by varying the slope of the droop characteristic, system operator can vary the power ratio between the two DC voltage controlling terminals. If the droop characteristic of the first VSC is considered to be fixed, the droop characteristic of the second VSC can be varied so that the relationship between their power is accomplished as [11]:

$$\frac{P_{dc1}}{P_{dc2}} \approx \frac{I_{dc1}}{I_{dc2}} = n = \frac{R_{dc2} + 1/k_2}{R_{dc1} + 1/k_1} \Rightarrow k_2 = \frac{1}{n/k_1 + n \cdot R_{dc1} - R_{dc2}} \tag{10}$$

where n is the power ratio and k is the slope of the droop controller.

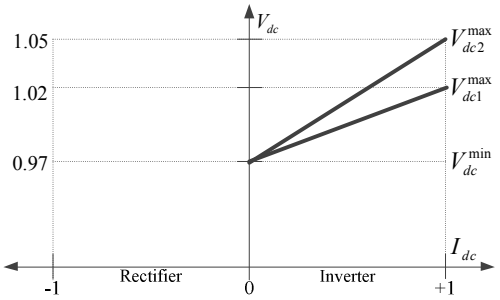

Fig. 10: MTDC droop controller for ratio control.

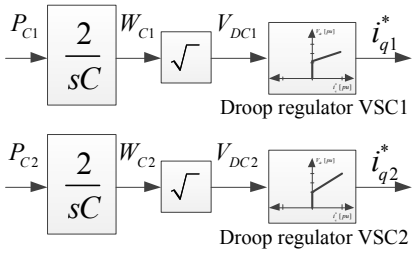

Fig. 11: Block representation of the ratio control strategy.

Priority Control

In this control strategy, one VSC terminal will have precedence over the other terminal for the power generated by the wind farms. This is accomplished by combination of two different direct voltage controllers. The first terminal, the one with the precedence, will control the DC voltage, by means of a PI regulator, until it reaches its rated capacity or a maximum power set point established by system operators. Thus, the second terminal will only start transmitting power once the first terminal has reached its limit [11]. A DC voltage droop controller is then provided to the second VSC terminal, so that it will receive all the remaining power that could not be transmitted through the first terminal.

When the power generated by the wind farms exceeds the capabilities of the first VSC terminal, it will have reached its rated current and, thus, it will no longer be capable of controlling the DC voltage in the MTDC network. As a consequence of the power unbalance, the DC voltage inside the system will start to increase. When the direct voltage inside the MTDC network will be greater than V_{dc2} (min), VSC terminal 2 will start transmitting power. Again, as was the case for the droop control strategy, the choice of V_{dc2}(min) and V_{dc2}(max) in Fig. 12, has to take into account the system design rules, such as the DC voltage ratings of the VSC stations and of the DC cables.

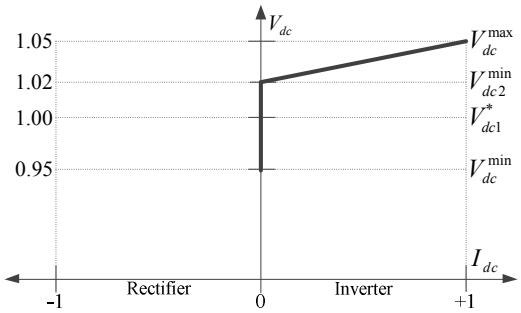

Fig. 12: MTDC droop controller for priority control.

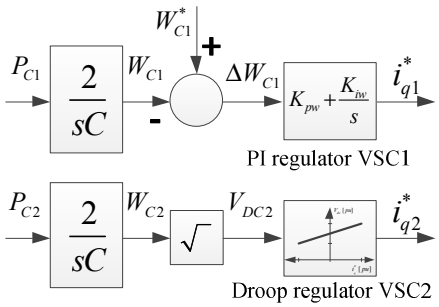

Fig. 13: Block representation of the priority control strategy.

Voltage Margin Method

The Voltage Margin Method was first proposed in 1999 by Nakajima and Irokawa [3]. In this control strategy each converter station in the system is given a marginally offset DC voltage reference [12]. This control scheme is dual to the current margin method proposed for controlling CSC-MTDC networks [13]. Similarly to the CSC-MTDC case, the voltage margin is defined as the DC voltage reference difference between the terminals. The 2-stage voltage margin method scheme is depicted below in Fig. 14 and its block representation is given in Fig. 15. The 2-stage scheme is more suited for multi-terminal DC systems, as it reduces the need for communication between the terminals and each converter receives a control structure such as the one shown in Fig. 15 [12].

Between the converter limit as a rectifier and a reference AC power (P_{ac}*), the VSC terminal will try to control the DC voltage at V_{dc}*(low) by means of the lower DC voltage PI regulator. If the network voltage is within V_{dc}*(low) and V_{dc}*(high), the VSC terminal will regulate the converter power to P_{ac}* by means of the active power PI regulator. Finally, if the network voltage increases, between P_{ac}* and the converter limit as an inverter, the VSC terminal will try to control the DC voltage at V_{dc}*(high) by means of the upper DC voltage PI regulator.

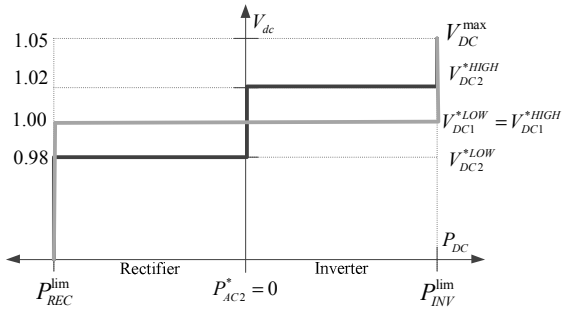

Fig. 14: Voltage margin method controller with two VSC terminals.

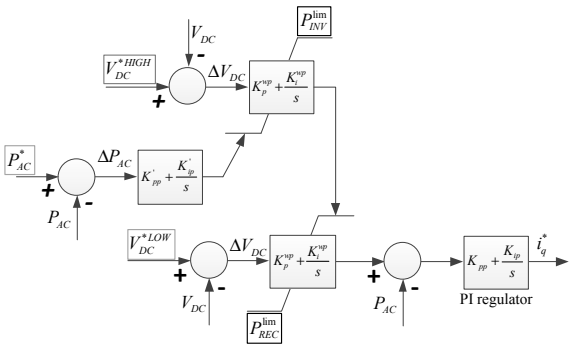

Fig. 15: Block representation of the voltage margin method controller.

Case Study

In order to test the different schemes which implement a distributed control strategy of the DC voltage inside MTDC networks, a system consisting of four nodes – two AC grids and two wind farms – is proposed. The AC grids and the wind farms are modelled as ideal voltage sources behind impedances. The base DC voltage is 400 kV (± 200 kV) and the system base power is 500 MVA. In the case study, the wind farms are considered to be producing power according to the order of events displayed in Table I.

Table I: Order of events in the 4-node MTDC Network.

Time [s]	0	0.50	1.00	1.50	2.00	3.00
WF 1 Power [pu]	0	0.50	0.50	0.80	0.80	0.50
WF 2 Power [pu]	0	0	0.40	0.40	0.80	0.40

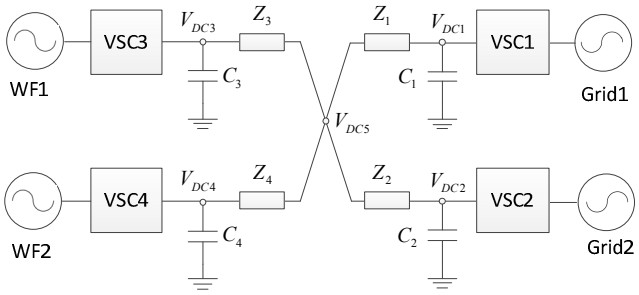

Fig. 16: MTDC Network with 4 nodes.

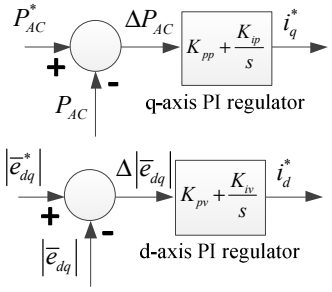

Fig. 17: Wind-farm side VSC controllers.

Results

For the different considered control methods in the case study, the direct voltage and the active power at all the VSC terminals are displayed in Fig. 18 in the appendix.

In the voltage droop control method, given that the VSC1 and VSC2 terminals have the same droop characteristic, the power produced by the wind farms is equally shared among the two stations. Since the droop control is equivalent to a proportional control, the dynamic behaviour of the active power is given by the inner current controller loop, which has fast dynamics. As a consequence, the changes in the direct voltage with the different operating points occur almost instantaneously. Extending the droop control method to MTDC networks with more terminals should be straightforward. The downside of the droop control method as presented, regards the fact that steering the power produced by the wind farms to a particular node in the network is not possible.

In the ratio control method the VSC1 and VSC2 terminals have different droop characteristics according to (12). In the case study, the power ratio (n) between the VSC1 and VSC2 terminals is n = 50/50 for $0 < t < 1$s, n = 70/30 for $1 < t < 2$s, n = 40/60 for $2 < t < 3$s and back to n = 50/50 for $t > 3$s. The simulation results show that the power division is not exactly equal the value established by the power ratio coefficient, however, the precision is high and above 95%. As it is the case for the droop control, the ratio control can be traced back to a proportional gain. However, in the ratio control, this proportional gain – equal to the inverse of the droop slope – is not constant. If the gain is made too high, i.e. the slope too low, the DC voltage can display an oscillatory or even have an unstable behaviour. A downside of the ratio control approach may be its expandability. It may be difficult to find an analytic expression for the case with more than two stations. In addition, the analytic expression depends on the resistance of the DC cables, which may vary, further affecting the method's accuracy [11].

In the priority control method the first VSC terminal will try to control the DC voltage at a pre-defined level until it reaches its full capacity. This behaviour can be clearly seen in the first two DC voltage transients, when the two wind farms start producing power, respectively at t = 0.5s and t = 1s. During the transients, the DC voltage initially rises to approximately 1.03 pu and is then re-established to its pre-defined level of 1 pu in approximately 200 ms. When the VSC1 terminal saturates at t = 1.5s, the VSC2 terminal starts receiving the exceeding power from the wind farms and the DC voltage varies according to the droop characteristic of the VSC2 terminal. Finally, at t = 3s, when the wind farms power is reduced, the VSC1 terminal comes out of saturation bringing back the DC voltage to its initial value of 1 pu and, thus, no more power is sent to the VSC2 terminal.

The priority control strategy is interesting for small MTDC networks where a specific country wishes to have precedence over the power produced by its wind farms and is willing to sell the exceeding power to neighbour countries. However, it is not clear how this control method can be extended to MTDC networks with a larger number of nodes. A solution could be to combined the priority control strategy with the ratio control strategy, but also in the latter expansion to MTDCs with higher number of nodes seems to be challenging.

The last control strategy to be considered in the case study is the voltage margin method. Among the methods compared this is the one with highest flexibility. In fact, the voltage margin method can be used to emulate the other control strategies presented, such as the ratio and priority controllers. A voltage margin scheme in which the VSC1 terminal has the priority over the VSC2 terminal is shown in the Fig. 15. The simulation results shown that the voltage margin method successfully implements the priority control strategy. With the aid of communication and knowledge of the power produced by the wind farms, it would also be possible to use the voltage margin method to implement the ratio control strategy by varying the VSC2 terminal active power reference, P_{ac2}*, accordingly.

However, the dynamic response of the voltage margin method was not as fast as the original priority controller and this effect can be clearly seen in the DC voltage response. While the other DC voltage strategies have shown voltage transients which were less than 5% the nominal voltage, for the voltage margin method these transients were somewhat higher, with the highest overvoltage being of 12% the nominal value. The way the method is constructed, by cascading several PI controllers, could be

related to the more sluggish response. Another downside of the voltage margin method, as implemented, is that only one VSC station is capable of controlling the system DC voltage at a time. Nonetheless, extending the voltage margin method to MTDC networks with a higher number of nodes should be easier to accomplish than for the ratio or priority controllers. However, with a limited DC voltage normal operating range, e.g. ±5% the nominal voltage, the maximum number of VSC terminals that can be controlled by the voltage margin method may be limited to avoid adverse interaction between the controls of each terminal due to possible too low voltage margins.

Conclusions

The table below reviews the characteristics of the analysed DC voltage control methods for MTDC networks.

Table II: Comparison of the different evaluated methods.

Control Method	Dynamic Response	Expandability	Flexibility	Communication requirement
Droop	High	Medium	Low	Low
Ratio	High	Low	Medium	Medium
Priority	Medium	Medium	Medium	Low
Voltage Margin	Low	High	High	Medium

To guarantee a secure and reliable DC grid operation in future large offshore multi-terminal networks it seems necessary to distribute the DC voltage control responsibility to more than one converter terminal. The best control strategy will be the one with good dynamic behaviour, high flexibility and expandability, and low communication requirements. No single control method analysed has shown all the requirements per se. Thus, as a conclusion from the results shown in Table II, a possible solution could be to combine the voltage margin method with the droop control strategy.

References

[1] Cigré: VSC Transmission, Working Group B4.37.
[2] Arrillaga J., Liu Y. H., Watson N. R.: Flexible power transmission: the HVDC options. Wiley & Sons, 2007.
[3] Nakajima T., Irokawa S.: A Control System for HVDC Transmission by Voltage Sourced Converters, in IEEE Power Engineering Society Summer Meeting, Edmonton, pp. 1113–1119, 1999.
[4] Kazmierkowski M., Krishnan R., Blaabjerg F.: Control in Power Electronics, Academic Press, 2002.
[5] Mohan N., Undeland T. M., Robbins W. P.:, Power Electronics: Converters, Applications and Design, Wiley & Sons, 1995.
[6] Harnefors L., Bongiorno M., Lundberg S.: Input-Admittance Calculation and Shaping for ControlledVoltage-Source Converters, IEEE Transactions OnIndustrial Electronics, Vol. 54, pp. 3323–3334, Dec. 2007.
[7] Zhang L., Harnefors L., Nee H.-P.: Interconnection of two very weak ac systems by vsc-hvdc links using power-synchronization control," IEEE Transactions on Power Systems, pp. 1-12, 2010.
[8] Lasseter R., Alvarado F., Adapa R.: Expandable multiterminal dc systems based on voltage droop, IEEE Transactions on, vol. 8, 1993, pp. 1926-1932.
[9] Hendriks R.L., van der Meer A.A., Kling W.L.: Impact on System Stability of Different Voltage Control Schemes of Wind Power Plants Connected Through AC and VSC-HVDC Transmission, Proc. of the Nordic Wind Power Conference, Bornholm, 2009.
[10] Xu L., Williams B.W., Yao L., Bazargan M.: Control and Operation of Multi-Terminal DC Systems for Integrating Large Offshore Wind Farms, Proc. of the 7th International Workshop on Large-Scale Integration of Wind Power into Power Systems, Madrid, 2008.
[11] Xu L., Yao L., Bazargan M.: DC Grid Management of a Multi-Terminal HVDC Transmission System for Large Offshore Wind Farms, International Conference on Sustainable Power Generation and Supply, 2009.
[12] Livermore L., Liang J., Ekanayake J.: MTDC VSC Technology and its applications for Wind Power. [Online] http://www.supergen-networks.org.uk/publications. Last Accessed: May 2011.
[13] Kimbark E.W.: Direct Current Transmission, Wiley & Sons, New York, 1971.

Appendix: Simulation Results

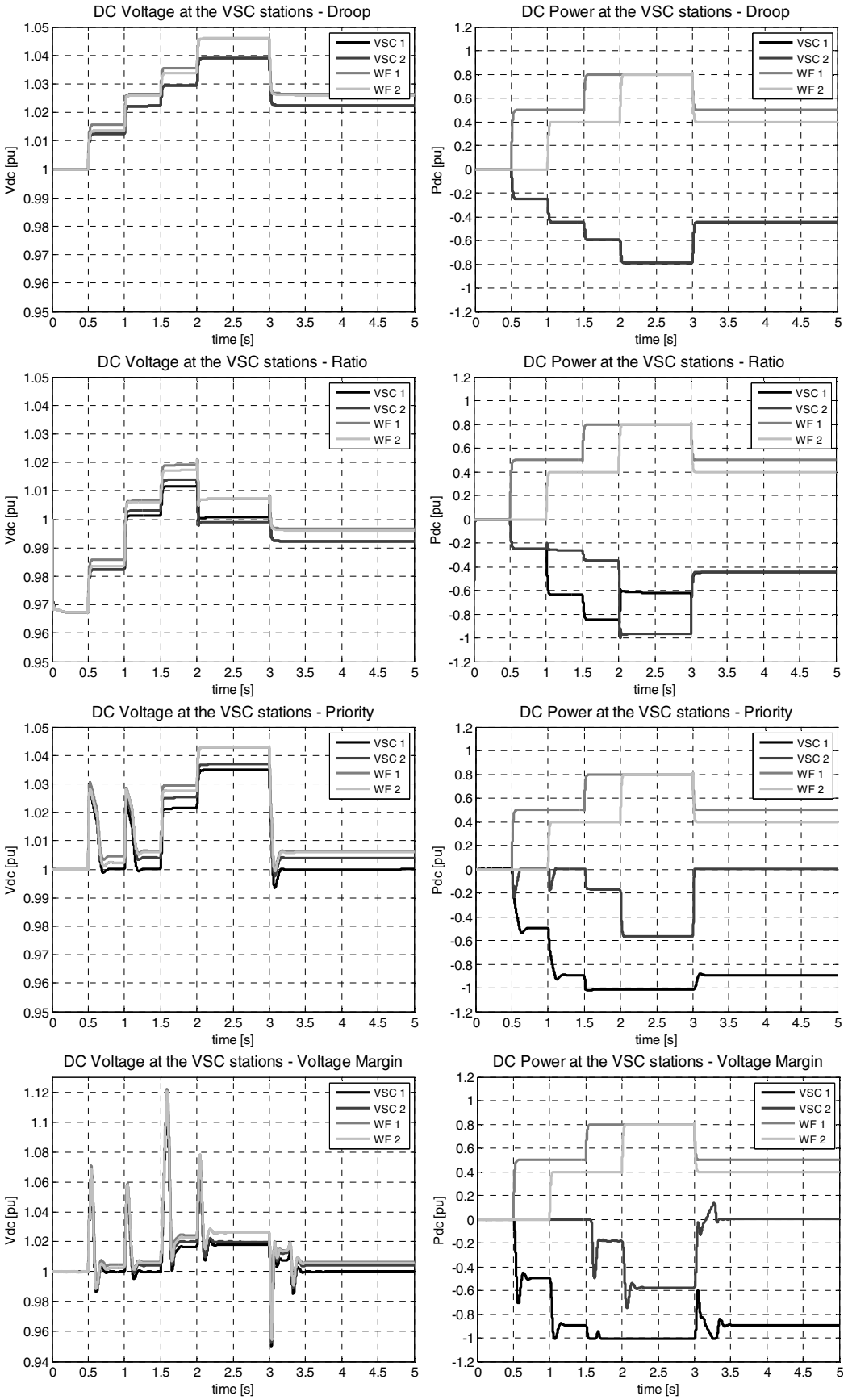

Fig. 18: Simulation results for the different DC voltage control methods in the case study.